

Formation and Dissolution of Single and Mixed Zn and Ni Precipitates in Soil: Evidence from Column Experiments and Extended X-ray Absorption Fine Structure Spectroscopy

ANDREAS VOEGELIN* AND
RUBEN KRETZSCHMAR

Institute of Terrestrial Ecology, Department of Environmental Sciences, Swiss Federal Institute of Technology, Grabenstrasse 3, CH-8952 Schlieren, Switzerland

The stability and the formation and dissolution kinetics of mixed trace metal precipitates in soils are currently unknown. The objective of this study was to investigate slow sorption and release processes of Zn and Ni in a loamy soil using a combination of soil column experiments and extended X-ray absorption fine structure (EXAFS) spectroscopy. To investigate slow sorption processes, the soil material was packed into columns and leached with 5400 pore volumes of 10^{-2} M CaCl_2 solutions containing either ZnCl_2 (5.2×10^{-5} M) or NiCl_2 (5.2×10^{-5} M) or both ZnCl_2 and NiCl_2 (5.2×10^{-5} M each). The Zn and Ni concentrations in the column effluents were monitored. The metal breakthrough curves showed that slow sorption processes lead to metal retention, whereby Zn was more strongly retained than Ni. In the experiment with both Zn and Ni present, amounts of Zn and Ni similar to those in the experiments with either Zn or Ni alone were retained. Analysis of soil samples by EXAFS spectroscopy showed that layered double hydroxide (LDH)-type precipitates had formed in all columns and that a mixed ZnNi-LDH had formed in the presence of both Zn and Ni. The dissolution of those precipitates under acidic conditions was assessed by subsequent leaching of the columns with a 10^{-2} M CaCl_2 solution at pH 3.0 (~3000 pore volumes). When only Zn was present, 95% of the retained Zn was leached at pH 3. In contrast, only 23% of the retained Ni was leached in experiments with Ni alone. When Zn and Ni were present, 90% of the retained Zn and 87% of the retained Ni were released upon acidification. EXAFS analysis revealed that the LDH phases in the Zn experiment and the Zn–Ni experiment had been completely dissolved, while the LDH phase formed in the Ni experiment was still present. The higher resistance of Ni-LDH against dissolution at low pH could also be shown in dissolution studies with synthetic Zn-LDH, Ni-LDH, and ZnNi-LDH. Our results suggest that the individual rates at which Zn and Ni cations enter into the LDH structure determine the composition of the mixed ZnNi-LDH precipitate, and that the LDH

composition determines the rate at which the LDH phase dissolves under acidic conditions.

Introduction

Zinc and nickel are essential micronutrients for plants and animals. At elevated concentrations, however, they exert toxic effects on plants and microorganisms and may lead to a decrease in plant growth and soil fertility (1). The bioavailability and mobility of Zn and Ni in soils depend to a large degree on their chemical speciation. Both elements may adsorb to organic soil components and soil mineral surfaces (clay minerals, (hydr)oxides of Fe, Mn, and Al, carbonates). At near-neutral to alkaline pH values, slow sorption phenomena are observed for many trace metals, leading to a steady decrease in metal availability with time. Processes causing this behavior include the diffusion of metals into the interior of soil aggregates and microporous minerals and the formation of surface precipitates (2, 3). Using extended X-ray fine structure (EXAFS) spectroscopy, the formation of metal precipitates on mineral surfaces was extensively studied in recent years. Zinc and nickel were found to exhibit a similar behavior, forming metal hydroxides (4–6), mixed metal–Al layered double hydroxides (LDHs) (4, 7–11), or phyllosilicate-type precipitates (12–14) at near-neutral to alkaline pH. Formation of Zn-LDH and Ni-LDH precipitates was also reported from sorption studies on whole soil material and clay size isolates (15, 16). EXAFS studies on the speciation of Zn in soils contaminated from smelter emissions confirmed the formation of Zn-LDH and Zn-phyllosilicate precipitates under field conditions (17, 18).

While the insight into the diversity of trace metal speciation and the formation of metal-bearing precipitates in soils is rapidly expanding by the use of advanced spectroscopic techniques, the link of those results to the chemical reactivity and availability of trace metals is still not fully established. Thermodynamic data on the stability of trace metal LDH and phyllosilicate precipitates are still scarce (12, 19–21). The formation of trace metal precipitates in soils is also likely governed by kinetic factors such as the supply of Al and Si from the weathering of primary minerals rather than by thermodynamic equilibria (8, 22). Studies on Ni sequestration in model systems report an increasing stability of Ni precipitate phases with time as determined by repeated batch extraction using organic ligands or acidified solutions (22–25). One explanation was that initially formed Ni-LDH was increasingly stabilized by silicate-for-nitrate exchange in the interlayer. A limited number of studies thus far elucidated the effect of the presence of several sorbent phases or of organic molecules on the sequestration of Ni in mineral suspensions (24, 26–29).

One factor that has not been systematically addressed in previous studies is the simultaneous presence of several interacting trace metal cations and its influence on metal sequestration in precipitate phases. In a previous column study on Zn, Ni, and Co retention and release in a soil material, we found that Zn was incorporated into an LDH-type phase, which likely also contained Ni and Co (15). This phase was readily dissolved upon acidification of the soil to pH 3.0, leading to the release of Zn, Ni, and Co. For Ni, this finding was in some contrast to the relative stability of Ni-LDH phases reported in other studies (22–25). This suggests that trace metal precipitate formation and stability in soils may differ between single-metal and mixed-metal systems. To test this hypothesis, the objectives of the present study were (i) to

* Corresponding author phone: +41-44-6336147; fax: +41-44-6331118; e-mail: voegelin@env.ethz.ch.

investigate the retention of Zn and Ni in chromatographic soil columns both in single- and mixed-metal systems, (ii) to study the subsequent Zn and/or Ni release due to cation exchange and acidification reactions, and (iii) to relate the retention and release of Zn and Ni to their solid-phase speciation as inferred from EXAFS spectra recorded on Ca-exchanged and acidified soil samples.

Experimental Section

Soil. The soil material was collected from the B-horizon (15–25 cm sampling depth) of an acidic loamy soil in northern Switzerland (Riedhof, aquic dystric Eutrochrept). The same soil has been used previously in a study on Cd, Zn, and Ni sorption and reactive transport modeling (30) and in a study on the formation and release of a mixed ZnNiCo-LDH precipitate (15). The air-dried soil was sieved to separate the size fraction 63–400 μm , which consisted of small aggregates containing 0.37 g/g sand, 0.47 g/g silt, 0.16 g/g clay, and 9 g/kg organic carbon. The soil has a mixed clay mineralogy (illite, vermiculite, Al-hydroxy-interlayered clay minerals, kaolinite, chlorite) as determined by X-ray diffraction (XRD) analysis. A six-step sequential extraction procedure was used to characterize Al, Fe, and Mn in the soil material (31, 32). Experimental details and complete results are provided in the Supporting Information. A 23 mmol/kg concentration of Al was found to be extractable with unbuffered 1 M NH_4NO_3 (“exchangeable fraction”, fraction 1). In later steps, 60 mmol/kg Al and 63 mmol/kg Fe were extracted using 0.2 M NH_4 -oxalate at pH 3.25 (“amorphous iron oxides”, fraction 5), and 99 mmol/kg Al and 114 mmol/kg Fe were extracted with 0.1 M ascorbic acid + 0.2 M NH_4 -oxalate at pH 3.25 and 96 °C (“crystalline iron oxides”, fraction 6). Total Zn and Ni contents of the untreated soil as determined by X-ray fluorescence (XRF) spectroscopy (Spectro X-Lab 2000) are 0.91 mmol/kg Zn (60 mg/kg) and 0.51 mmol/kg Ni (30 mg/kg).

Column Breakthrough and Release Experiments. Chromatographic glass columns (Omni) with an inner diameter of 1 cm were uniformly packed with 1.5 g of dry soil. The resulting soil columns were 1.7 cm long, with a pore volume of 0.75 mL and a packing density of 2.0 g of soil/mL of pore volume. After packing, a stream of CO_2 gas was passed through the columns to displace the enclosed air. The CO_2 gas readily dissolves after the water percolation is started with an HPLC pump, thereby ensuring complete water saturation of the pore space. All solutions were first passed through a degasser and then through the columns in an upward direction. The following percolation scheme was applied: (Step 1) Preconditioning of the columns with 1300 pore volumes of 1 M CaCl_2 at a flow rate of 1 mL/min (0.75 min/pore volume). (Step 2) Conditioning of the column with 2670 pore volumes of a 10^{-2} M CaCl_2 solution buffered to pH 7.4 (1 mM HEPES buffer and 0.5 mM NaOH, 0.75 min/pore volume). (Step 3) Rapid metal loading with solutions containing 5.2×10^{-5} M ZnCl_2 (column A, Zn-only single-metal experiment), 5.2×10^{-5} M NiCl_2 (column B, Ni-only single-metal experiment), or 5.2×10^{-5} M ZnCl_2 and 5.2×10^{-5} M NiCl_2 (column C, ZnNi mixed-metal experiment) in a background electrolyte of 10^{-2} M CaCl_2 buffered to pH 7.4 (1 mM HEPES, 0.5 mM NaOH). Each column was rapidly loaded with 1320 pore volumes at a flow rate of 0.75 mL/min (taking 22 h, 1.0 min/pore volume). Note that the metal concentrations in the influent solutions were chosen to be at least 1 order of magnitude lower than the solubility limits of the respective metal (hydr)oxides at pH \approx 7.4 (lowest log K for M-(hydr)oxide $\rightleftharpoons \text{M}^{2+} + 2\text{OH}^-$, from ref 33: -16.7 for ZnO and -15.2 for Ni(OH) $_2$). (Step 4) After 1320 pore volumes, the flow rate was decreased to 0.1 mL/min. If the uptake of Zn and Ni is rate-limited, the reduction of the flow rate would result in an increase of the fractions of Zn and Ni removed

from the solution and thus in an immediate reduction of the Zn and Ni concentrations in the effluent. Slow metal loading at 0.1 mL/min was continued over 4080 pore volumes (taking 21 days, 7.5 min/pore volume). (Step 5) Leaching with 1320 pore volumes of 10^{-2} M CaCl_2 (pH \approx 6) at a flow rate of 0.5 mL/min to remove exchangeable cations (1.5 min/pore volume). After the first 660 pore volumes, the flow was stopped for 6 h to check for kinetic effects. After the leaching with 10^{-2} M CaCl_2 was finished, the columns were disassembled and the soil material was dried at 40 °C. While 0.9 g of dry soil was kept for EXAFS analysis, the remaining 0.6 g was again packed into the chromatographic columns. (Step 6) In the final leaching step, the repacked columns were leached with 3000 pore volumes of 10^{-2} M CaCl_2 adjusted to pH 3.0 (with HCl) at a flow rate of 0.6 mL/min to release acid-extractable metals (taking 1500 min, 0.5 min/pore volume). The acidified soil material was dried at 40 °C. The effluent of the columns was sampled in 10 mL PE tubes using an automated fraction collector. Samples for Zn and Ni analysis were acidified with concentrated HCl (1%, v/v). The undiluted samples were measured using flame atomic absorption spectrometry (F-AAS; Varian Spectraa 220). Calibration standards prepared in 10 mM CaCl_2 were remeasured after every 10 samples.

The concentrations of Zn and Ni in the soil samples after Ca leaching, after acidification to pH 3.0, and in untreated soil were determined by HNO_3 extraction: Duplicate samples ($35\text{--}50 \pm 0.1$ mg) were extracted in 2.5 mL of 2 M HNO_3 for 2 h at 94 °C. The extracts were filtered through 0.2 μm nylon filters. Using F-AAS, Zn and Ni were analyzed at 10-fold and 100-fold dilution, respectively. The relative standard deviations for the concentrations of Zn and Ni in soils were $<5\%$.

Preparation of Zn-, Ni-, and ZnNi-Al LDH Reference Phases. The synthesis followed the procedure by Taylor (34). Briefly, solutions containing 20 mmol/L AlCl_3 together with 40 mmol/L ZnCl_2 or 40 mmol/L NiCl_2 or 20 mmol/L ZnCl_2 and 20 mmol/L NiCl_2 were titrated with 0.1 M NaOH to a pH of 6.5 under a N_2 atmosphere. The resulting precipitates were washed four times with deionized water. X-ray diffraction patterns of the powdered products are shown in the Supporting Information. They confirmed the formation of Zn- and Ni-LDH phases in the single-metal systems and showed that a mixed ZnNi-LDH phase had formed in the presence of Zn and Ni.

Dissolution of Zn-LDH, Ni-LDH, and ZnNi-LDH Reference Phases at pH 3.0. The kinetics of the dissolution of the Zn-LDH, ZnNi-LDH, and Ni-LDH reference phases were investigated at pH 3.0 (1 mM HCl) in 10 mM CaCl_2 . Experiments were run in triplicate. A 3.0–3.5 mg sample of the respective solid was added to 200 mL of solution, which was stirred in a glass beaker covered with a watch glass. Samples were collected at increasing time intervals (1.25–645 min for the Zn-LDH, 2.5–1361 min for the ZnNi-LDH, and 13–5700 min for the Ni-LDH), immediately filtered through 0.2 μm nylon filters, and acidified with 1% (v/v) concentrated nitric acid. The solutions were analyzed for Zn, Ni, and Al using inductively coupled plasma optical emission spectrometry (ICP-OES). Calibration standards were run after every 20 samples, and each set of 20 samples contained blanks and control samples of known concentration. Final pH values in the suspensions were 3.08 (Zn-LDH), 3.13 (ZnNi-LDH), and 3.10 (Ni-LDH).

EXAFS Measurements and Analysis. Zn K-edge (9659 eV) and Ni K-edge (8333 eV) EXAFS spectra were measured for soil samples and reference phases. Spectra for the Ca-treated soil samples, for Ni in the acid-leached Ni column, and the reference spectra were collected at beamline X-11A at the National Synchrotron Light Source (NSLS), Upton, NY. The electron storage ring was operated at 2.5 GeV, and the beam current varied between 300 and 100 mA. The beamline

monochromator consisted of two parallel Si(111) crystals. The monochromator was detuned by 25% to reduce higher harmonics. The soil samples were run as powders mounted on a coldfinger cooled with liquid N₂. Spectra in fluorescence mode were recorded using a Stern–Heald-type detector filled with Ar gas and equipped with a Cu-3 filter for Zn and a Co-3 filter for Ni (35). About 4–6 scans were collected and averaged for each soil sample to achieve an acceptable signal-to-noise ratio. Three scans in transmission mode were measured for reference spectra diluted in boron nitride. The spectrum on Zn in the Zn column after pH 3.0 leaching was measured at the Rossendorf beamline (ROBL) at the European Synchrotron Radiation Facility (ESRF), Grenoble, France. The electron storage ring was operated at 6 GeV with a beam current of 200 mA. The beamline monochromator consisted of two parallel Si(111) crystals equipped with two mirrors to reduce the higher harmonics (36). The sample was prepared as a PE pellet and measured in a He cryostat at 30 K using a 13-element Ge solid-state detector. The spectrum was obtained by averaging seven scans. The spectra for Zn and Ni in the mixed column after acidification were measured at the X-ray absorption spectroscopy (XAS) beamline at the Angstromquelle Karlsruhe (ANKA), Germany. The ring was operated at 2.5 GeV and a beam current of 130 mA. The Si(111) monochromator was detuned by 40% using a software-controlled monochromator stabilization. For both samples, three scans were measured at room temperature using a five-element solid-state detector.

Data analysis was carried out using the program WinXAS 3.1 (37). Averaged scans were normalized using a first-order polynomial in the pre-edge region and a second-order polynomial for the EXAFS region. The E_0 of the K-edge was determined from its inflection point (second derivative). The EXAFS signal was extracted using a cubic spline fit. The k range from 2 to 10 Å⁻¹ was Fourier transformed, and the r range from 0.8 to 3.3 Å was used to calculate the Fourier-filtered back-transform. Single-shell fitting was done in r space using Zn–O, Zn–Zn, Zn–Al, Ni–O, Ni–Al, and Ni–Ni paths calculated with FEFF 7 on the basis of the structure of hydroxalcalcite (38). The amplitude reduction factor S_0^2 was fixed at 0.85 (13, 39). In a first step, the first shell (Zn–O or Ni–O, fit range $r = 0.8–2.15$ Å) was fit (coordination number, distance, Debye–Waller factor, and ΔE_0) using the respective theoretical path. The first-shell parameters and ΔE_0 were then fixed, and the fit range was extended to 0.8–3.3 Å. The second shell was fit with either the M–M or the M–Al path (M = Zn or Ni). Only the coordination number and the distance R_{M-X} were adjusted during the fit. The Debye–Waller factor for the second shell was fixed to 0.008 Å². This value was found suitable in preliminary fits with floating Debye–Waller factors and is similar to factors that have previously been used for fitting second shells of Zn and Ni in layered species (8, 13). The deviation between the fitted and the experimental spectra is given by the normalized sum of the squared residuals $\chi_{res}^2 = \sum_i((k^3\chi_{exp} - k^3\chi_{fit})^2) / \sum_i((k^3\chi_{exp})^2)$.

Results and Discussion

Metal Sorption. The breakthrough curves of Zn and Ni (influent concentrations $c_0 = 5.2 \times 10^{-5}$ M) at pH 7.4 are presented in Figure 1. In the experiments with either Zn or Ni (Zn-only and Ni-only single-metal experiments, filled symbols), the curves clearly exhibit a stronger retention of Zn than of Ni. After 1300 pore volumes, the effluent concentration of Ni approached 90% of the influent concentration, while the normalized effluent concentration of Zn reached only 30%. The subsequent reduction in flow rate from 0.75 to 0.1 mL/min resulted in a pronounced decrease in both Ni and Zn concentrations in the effluent. This demonstrates that the uptake of Zn and Ni at this stage was rate-limited. Following the sharp decrease in effluent con-

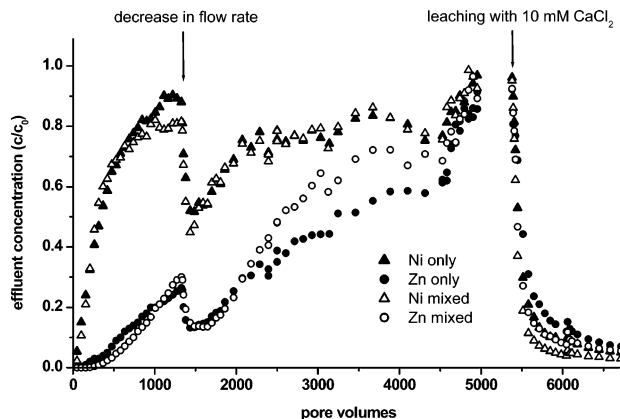


FIGURE 1. Breakthrough of Zn and Ni in single (solid circles and triangles, respectively) and mixed (open circles and triangles, respectively) column experiments in 10 mM CaCl₂ buffered to pH 7.4 and subsequent release by leaching with unbuffered 10 mM CaCl₂ (influent concentration $c_0 = 5.2 \times 10^{-5}$ M).

TABLE 1. Amounts of Zn and Ni Retained and Releases in Single- and Mixed-Metal Column Experiments

	Zn (single)	Ni (single)	Zn (mixed)	Ni (mixed)	Zn + Ni (mixed)
Millimoles per Kilogram					
total sorbed ^a	73.8	37.6	68.8	35.9	104.7
Ca-exchanged ^b	6.7	5.3	4.9	3.5	8.4
pH 3 leached ^c	63.6	7.6	57.3	28.1	85.4
residual ^d	3.5	24.8	6.6	4.2	10.8
Percent of Total Sorbed					
Ca-exchanged	9.1	14.0	7.1	9.9	8.1
pH 3 leached	86.1	20.1	83.3	78.5	81.6
residual	4.8	65.9	9.6	11.7	10.3
Percent of (Total Sorbed – Ca-Exchanged)					
pH 3 leached	94.8%	23.4%	89.7%	87.0%	88.8%
residual	5.2%	76.6%	10.3%	13.0%	11.2%

^a Sum of the Ca-exchanged amounts and of amounts retained after Ca leaching as determined by 2 M HNO₃ extraction. ^b Determined by integration of the release curve during Ca leaching. ^c Determined by the difference of the 2 M HNO₃ extractable amounts before and after pH 3 leaching. ^d Determined by 2 M HNO₃ extraction of residual soil (corrected for amounts extractable from untreated soil).

centrations upon the reduction of the flow rate, effluent concentrations steadily increased again. After about 4700 pore volumes, they rapidly increased to values close to the influent concentration, suggesting a decrease in the sorption rate. In the experiment where both Zn and Ni were simultaneously present (mixed-metal experiment, open symbols), the breakthrough curves of Zn and Ni closely resembled those from the single-metal systems, except that the concentration of Zn in the effluent increased more rapidly after 2000 pore volumes.

The total amounts of Zn and Ni retained in the columns are given in Table 1. About twice as much Zn as Ni was sorbed in the single- and mixed-metal column experiments. The total sorbed amounts of Zn and Ni were similar for single and mixed systems, suggesting that competitive sorption effects on metal sorption were overall small at the concentration levels used in this study.

Metal Release by Ca Exchange. Upon reacting the columns with Zn- and/or Ni-containing solutions, the soils were first leached with 10 mM CaCl₂ solution to monitor the release of adsorbed Zn and Ni exchangeable by Ca (Figure 1). During the leaching with unbuffered 10 mM CaCl₂, the effluent rapidly reached pH 6.5. The patterns of Zn and Ni in both the single and binary experiments resemble each

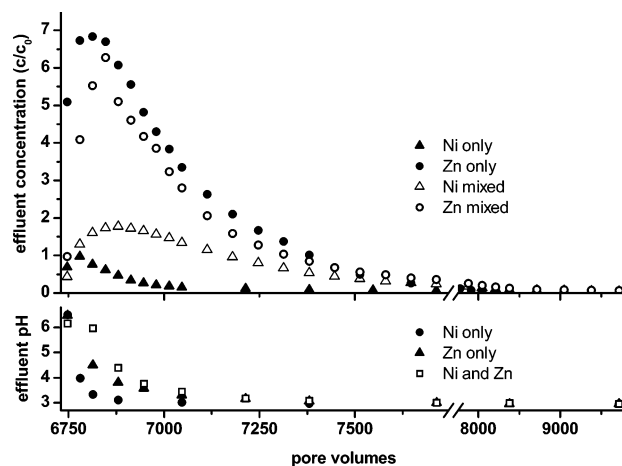


FIGURE 2. Release of Zn and Ni in single (solid circles and triangles, respectively) and mixed (open circles and triangles, respectively) column experiments during acidification at pH 3.0. The lower graph shows the breakthrough of the pH in the single-metal experiments with Zn and Ni (solid circles and triangles, respectively) and the mixed-metal experiment (open squares) ($c_0 = 5.2 \times 10^{-5}$ M, 0.5 min/pore volume).

other. However, 28% more Zn than Ni was released in the single-metal experiments, and 39% in the binary experiment, suggesting that more Zn than Ni had been adsorbed on cation exchange sites and that Zn was slightly preferred over Ni in the mixed-metal system. Competition of Zn and Ni for exchange sites is also reflected by the fact that the sum of Zn and Ni retained in the mixed-metal experiment was 30% smaller than the sum from the single-metal experiments (Table 1).

Metal Release due to Acidification. To study the mobilization of the remaining Zn and Ni during acidification of the soil, the Ca-extracted soil was subsequently leached with 10 mM CaCl_2 adjusted to pH 3.0. The respective elution curves are depicted in Figure 2. In the single-metal experiment with Zn, 95% of the nonexchangeable Zn was released during acidification (Table 1). In contrast, only 23% of the nonexchangeable Ni was released, while 77% resisted leaching with 3000 pore volumes of a 10 mM CaCl_2 solution at pH 3.0.

In the binary experiment with Zn and Ni, 90% of the remaining Zn was leached during acidification, i.e., slightly less than in the experiment with only Zn. The elution of Zn was also somewhat delayed compared to that of the Zn-only experiment. For Ni, an entirely different behavior was found in the ZnNi than in the Ni-only experiment: 87% of the remaining Ni was now released during acidification, in contrast to only 23% in the Ni-only experiment. These observations are also reflected in the breakthrough of the pH front: In the experiment with only Ni, the effluent pH most rapidly reached pH 3.0, reflecting the small amount of Ni released from the soil. In the Zn-only experiment, on the other hand, more time was needed until the effluent reached pH 3.0, reflecting the much larger amount of Zn released. The breakthrough of the pH front was most strongly retarded in the mixed-metal system, due to the release of Zn and Ni upon acidification. The results from the acidification step show that, even though the breakthrough front for Ni in the mixed-metal experiment looked very similar to that of the experiment with only Ni, the phase that formed was significantly destabilized by the presence of Zn. For Zn, on the other hand, the presence of Ni resulted in a slight reduction in the amount leached (Table 1).

Zn and Ni EXAFS Spectroscopy. Ni and Zn K-edge EXAFS data for the soil samples and for LDH references are shown in Figure 3. The k^3 -weighted χ functions of the EXAFS region, their Fourier-transforms, the Fourier-filtered back-transforms

over the r range 0.8–3.3 Å, and two-shell fits are plotted. Sample descriptions and fit parameters are provided in Table 2. The Ni and Zn spectra collected after the samples were leached with CaCl_2 compare well to the spectra of the synthetic single and mixed LDH phases. They reveal the same combination of spectral details as the LDH references, i.e., the weak splitting at 3.7 Å⁻¹, the shoulder at 5.1 Å⁻¹, and the beat pattern at 8.0 Å⁻¹ (6). Neither reference spectra of phyllosilicate-type nor of hydroxide-type precipitates show the same combination of characteristic spectral features in k space (see the Supporting Information for a comparison of Fourier-filtered EXAFS spectra of different layered precipitates and of Ca-leached soil samples). Thus, from the close match of the χ spectra of Zn and Ni in the Ca-leached soil samples and the spectra of synthetic Zn- and Ni-LDH phases, we conclude that Zn and Ni in those samples are predominantly present in LDH-type precipitates.

For the mixed-metal column experiment, the question remains whether Zn and Ni are present in a single type of precipitate or whether two separate precipitates had formed. From the similar release curves of Zn and Ni during acidification of the mixed-metal column (Figure 2), the formation of a single type of mixed-metal precipitate can be postulated (15). This would also be consistent with the synthesis of a mixed ZnNi-LDH phase from Zn- and Ni-containing solutions (see XRD spectra of the LDH reference phases in the Supporting Information). Further indications may be obtained from the two-shell fits of the Ca-exchanged soil samples and the LDH reference phases (Table 2, Figure 3). Fitted first-shell coordination numbers are always larger than 6, which would be the expected value for Zn or Ni in octahedral coordination. This may be due to the choice of a too low amplitude reduction factor ($S_0^2 = 0.85$) or, more likely, due to the simultaneous fitting of the coordination number and Debye–Waller factor, which are correlated. However, fits with first-shell coordination numbers fixed to 4.5, 6, and 7.5 showed that the fitted first-shell distances varied by less than 0.02 Å. The first-shell Ni–O and Zn–O distances in the Ca-treated soil samples are slightly shorter than for the respective reference phases. For the fitting of the second shell, only metal–metal interactions were considered. The Al present at a distance similar to that of the metal and the contribution from six O atoms at ~3.6 Å in the LDH structure were not considered in order to constrain the fit. Therefore, and also because the Debye–Waller factor of the second shell was fixed to 0.008 Å², the coordination numbers of the second shells are only rough estimates. On the other hand, fits with Debye–Waller factors fixed to values of 0.006 and 0.010 Å² caused less than a 0.005 Å difference in the fitted second-shell distances. Because the Al at a similar distance was not included in the fit, these distances represent weighted distances rather than the true metal–metal distances. However, we expect similar trends in second-shell distances with changing precipitate structure in soil samples and reference phases, since all spectra were fitted in a consistent way. As for the first shell, second-shell distances are shorter in the Ca-treated soil samples than in the respective reference phase, which might indicate a higher crystallinity of the synthetic precipitates than of the precipitates in soil. Since Ni is a smaller ion than Zn, Ni–Ni distances are shorter than Zn–Zn distances. Shell fitting does not allow distinguishing between Zn and Ni in the second shell of Zn and Ni in the mixed-metal phase. However, from the distances obtained for the single-metal Ni-LDH and Zn-LDH reference phases (3.081 Å for Ni–Ni and 3.131 Å for Zn–Zn), a weighted arithmetic average distance of 3.108 Å can be calculated for a randomly mixed ZnNi-LDH (containing Zn and Ni in a molar ratio of 53:47). This compares to the fitted distances of 3.114 Å for Ni–Ni and 3.106 Å for Zn–Zn. Thus, the second-shell fit of the LDH reference

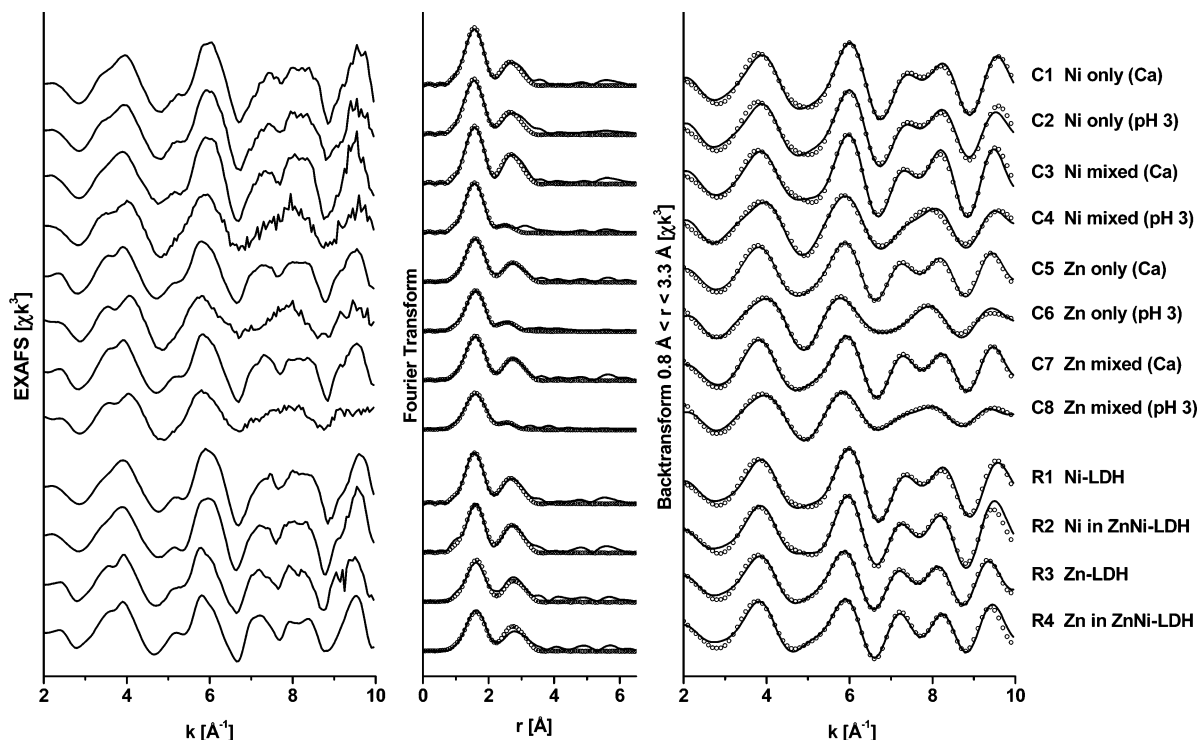


FIGURE 3. EXAFS K-edge $\chi^2 k^2$ spectra and their Fourier transforms and back-transforms for $0.8 \text{ \AA} < r < 3.3 \text{ \AA}$. Black solid lines represent experimental data, open circles single-shell fits involving the first and second shells. Fit results are provided in Table 2.

TABLE 2. Zn and Ni K-Edge EXAFS Fit Results ($S_0^2 = 0.85$) for Spectra from Column Soil Samples and Reference Phases

sample label	description	M-O			X^c	M-X			ΔE_0^d (eV)	$\chi_{res}^2 e$ (%)
		CN _{Mo} ^a	R (Å)	σ^2 ^b (Å ²)		CN _{MX} ^a	R (Å)	σ^2 ^b (Å ²)		
(C1) Ni single (Ca)	after Ca exchange	7.07	2.054	0.0053	Ni	3.89	3.071	0.008	-3.2	7.84
(C2) Ni single (pH 3)	after acidification	7.13	2.049	0.0056	Ni	3.76	3.071	0.008	-4.2	9.98
(C3) Ni mixed (Ca)	after Ca exchange	6.34	2.057	0.0039	Ni	4.96	3.095	0.008	-3.2	8.57
(C4) Ni mixed (pH)	after acidification	6.89	2.061	0.0064	Al	2.03	2.967	0.008	-3.2	10.41
(C5) Zn single (Ca)	after Ca exchange	6.92	2.075	0.0091	Zn	3.65	3.106	0.008	2.1	4.68
(C6) Zn single (pH)	after acidification	6.02	2.065	0.0087	Al	2.27	3.052	0.008	3.6	6.80
(C7) Zn mixed (Ca)	after Ca exchange	7.04	2.074	0.0092	Zn	4.06	3.093	0.008	2.5	2.91
(C8) Zn mixed (pH)	after acidification	6.82	2.071	0.0112	Al	1.87	2.989	0.008	4.0	7.39
(R1) Ni-LDH	Ni in Ni-Al LDH	6.47	2.063	0.0056	Ni	4.25	3.081	0.008	-2.7	6.62
(R2) Ni in ZnNi-LDH	Ni in mixed ZnNi-Al LDH	6.57	2.076	0.0065	Ni	4.73	3.114	0.008	-1.3	7.90
(R3) Zn-LDH	Zn in Zn-Al LDH	6.34	2.091	0.0086	Zn	4.02	3.131	0.008	3.5	5.63
(R4) Zn in ZnNi-LDH	Zn in mixed ZnNi-Al LDH	7.50	2.094	0.0116	Zn	4.67	3.106	0.008	2.9	5.45

^a Coordination number. ^b Debye-Waller factor, fixed to 0.008 \AA^2 for the second shell. ^c Neighboring atom used to fit the second shell. ^d Energy shift. ^e Normalized sum of the squared residuals of the fit, $\chi_{res}^2 = \sum_i ((k^2 \chi_{exp} - k^2 \chi_{fit})^2) / \sum_i ((k^2 \chi_{exp})^2)$.

spectra demonstrates that, in a mixed ZnNi-LDH, the Zn-metal and Ni-metal distances are similar; i.e., the Zn-metal distance is shorter than the Zn-Zn distance in the pure Zn-LDH, and the Ni-metal distance is longer than the Ni-Ni distance in the pure Ni-LDH. Considering the molar ratio of Zn and Ni retained in the column experiment with both Zn and Ni (67:33; Table 1) and using the Zn-Zn (3.106 Å) and Ni-Ni (3.071 Å) distances obtained for the column experiments with either Zn or Ni (Table 2), a weighted average distance of 3.094 Å can be calculated for the randomly mixed precipitate. This value compares favorably to the fitted values of 3.093 Å for Zn-metal and 3.095 Å for Ni-metal. These considerations thus provide spectroscopic evidence for the formation of a mixed ZnNi precipitate of LDH type in the mixed-metal experiment, in agreement with the observed simultaneous leaching of Zn and Ni during acidification.

The spectrum of Ni from the single-metal experiment after pH 3.0 leaching looks similar to the spectrum after Ca exchange, and fit parameters compare well. This demon-

strates that it is indeed the Ni-LDH precipitate which resisted the acidification of the soil to pH 3.0. In contrast, the spectra of Zn from the single-metal and mixed-metal experiments as well as the spectrum of Ni in the mixed-metal experiment after acidification are clearly different from the spectra obtained after Ca exchange (Figure 3). Thus, most of the Zn-LDH and the mixed ZnNi-LDH formed in the soil was dissolved during acidification. The second shell of the Zn spectra collected after acidification could not be fit with a heavy atom (Zn). Instead, Al at a distance of 3.052 Å (Zn only) or 2.989 Å (Zn mixed) provided a reasonable fit (Table 2). The difference in the fitted Zn-Al distances may be due to minor contributions from other Zn species with different second shells (Zn from residual Zn-LDH, Fe and Mn from Zn adsorbed to iron and manganese oxides), which were not considered in the fit. Also Ni in the mixed column after acidification had to be fit with Al as a second neighbor, resulting in a Ni-Al distance of 2.967 Å. These distances and the light type of second neighbor atom suggest that a major

fraction of the Zn resistant to acidification was located in a gibbsite-type sheet (4, 40, 41). Association of Zn with gibbsite is not likely because gibbsite dissolves at pH 3.0 and because the expected Zn–O distance would be around 2.02 Å due to a mixing of tetrahedral and octahedral coordination (4). Alternatives include the incorporation of Zn and Ni into the gibbsite-like sheets of lithiophorite or Al–hydroxy-interlayered clay minerals (40, 41). From the total Mn content of the soil (14.5 mmol/kg), 11.2 mmol/kg could be extracted in a six-step sequential extraction procedure (see the Supporting Information for details). Even if this entire amount were present as lithiophorite and assuming a maximum uptake of one Zn or Ni atom per three Mn atoms, lithiophorite could account at best for 3.7 mmol/kg metals retained after acidification, i.e., for less than 30% of the sum of residual Zn and Ni (Table 1). Thus, lithiophorite is not likely to be the major host mineral for residual Zn and Ni. XRD on the oriented clay fraction on the other hand confirmed the presence of HIM in this soil material (partial collapse of the XRD peak at 14 Å to 10 Å upon heating the K-saturated clay fraction to 350 °C). Therefore, considering the chemical composition and clay mineralogy of the soil material, we expect that Zn and Ni retained in the Zn-only and mixed-metal experiments after acidification are mainly incorporated in Al–hydroxy-interlayered clay minerals rather than in lithiophorite.

Precipitate Formation in Single- and Mixed-Metal Experiments. In the single-metal column experiments, more Zn than Ni was retained in a precipitate of LDH type. In the mixed-metal experiment, the Zn and Ni sorption was only slightly lower and a mixed LDH was formed rather than two single-metal LDHs. Thus, it appears that Zn and Ni precipitated at individual rates that were almost the same for the single-metal and the mixed-metal experiments and thereby determined the amount and composition of the resulting precipitate phase.

Numerous studies on the sorption of Zn, Ni, and Co in mineral suspensions report that the rate and extent of LDH formation were related to the rate of Al release from the dissolution of mineral phases (5, 7, 10, 11, 28, 42–45). The similar amounts of Zn and Ni retained in the single- and mixed-metal column experiments suggest that the extent of LDH formation was not limited by the amount of available Al. This is supported by the amounts of oxalate- and oxalate/ascorbate-extractable Al in the soil (60 and 99 mmol/kg, respectively; see the Supporting Information for details), which are both higher than the amount needed to precipitate 85 mmol/kg Zn + Ni in the mixed-metal experiment assuming the formation of a 2:1 metal–Al LDH precipitate. However, the kinetics and thermodynamics of Al supply might still control the rate of LDH formation. Studies on the adsorption and surface precipitation of Zn, Ni, and Co on alumina showed that the dissolution of the alumina was promoted by the presence of the metal cations (7, 42, 43). To date, no comparative study on the effects of Zn, Ni, and Co cations on Al release from alumina is available. Our column data suggest that Zn is more efficient than Ni in promoting Al release from Al-containing minerals for subsequent LDH formation. The similar breakthrough curves and the only slightly lower amounts of Zn and Ni retained in the mixed-metal experiment than in the single-metal experiments further indicate that the effects of Zn and Ni on Al release add up in the mixed system.

The stability of the resulting LDH precipitate is one factor that may drive Al release (42, 43). On the basis of a mechanical mixture model proposed for the prediction of LDH solubilities (19) and considering the solubility constants of Ni(OH)₂ (log *K* = –15.2 for Ni(OH)₂ ⇌ Ni²⁺ + 2OH[–]) and Zn(OH)₂ (log *K* = –16.2) (33), Zn-LDH would be expected to be more stable than Ni-LDH. This is in agreement with stability constants

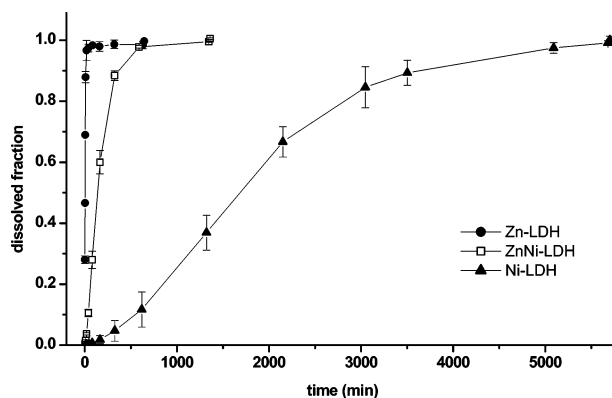


FIGURE 4. Dissolution of Zn-LDH, ZnNi-LDH, and Ni-LDH reference phases in 10 mM CaCl₂ adjusted to pH 3.0 (3.0–3.5 mg in 200 mL). The dissolved fraction was calculated by dividing the measured dissolved concentration of Zn, Zn + Ni, and Ni by the respective total amount in solution. Symbols and error bars indicate the average and standard deviation from three replicates, respectively.

of Zn- and Ni-LDH determined by base titration of metal solutions (20). Thus, the larger extent of Zn than Ni precipitation in the single-metal experiments correlates with a higher stability of Zn-LDH than of Ni-LDH.

From Ni and Co sorption studies on alumina, it was postulated that the release of Al from alumina was promoted by the adsorbed cations (42). In this case, Al release and LDH precipitation rates might be expected to increase with increasing amounts of adsorbed cations. Since Zn adsorbs more strongly to aluminum (hydr)oxide surfaces than Ni (46, 47), Zn-LDH would be expected to precipitate more rapidly than Ni-LDH. The expected trend thus correlates to the precipitated amounts of Zn and Ni in the column experiments. Note that in the column experiments, also the Ca-exchangeable amounts of Zn and Ni indicated a stronger adsorption of Zn than of Ni.

In a previous study on the simultaneous sorption of Zn, Ni, and Co to the same soil material, we found that a mixed LDH had formed and that the precipitated amounts decreased in the order Zn > Ni > Co (15). For Zn and Ni, these findings were confirmed by the mixed-metal experiment in the present study. Regarding the lower extent of Co precipitation, this result also correlates with the properties discussed above. The solubility of Co(OH)₂ (log *K* = –14.9) (33) is higher than that of Ni(OH)₂, suggesting a lower stability of the Co-LDH than the Ni-LDH (19), in agreement with experimental findings (20). On the other hand, Co also adsorbs less strongly to aluminum (hydr)oxide than Ni and Zn (46). Thus, the above discussion of possible factors affecting LDH precipitate formation also holds for Co.

Dissolution of Synthetic and Soil-Formed LDH Precipitates at pH 3.0. The EXAFS data show that the structures of the Zn, ZnNi, and Ni precipitates formed in soil columns are similar to the structures of the corresponding synthetic Zn-LDH, ZnNi-LDH, and Ni-LDH. It was therefore of interest to test if the dissolution behavior of the synthetic LDH phases at pH 3.0 compares to the release of Zn and Ni in the single- and mixed-metal column studies. A dissolution experiment at pH 3.0 in 10 mM CaCl₂ was therefore run with the Ni and Zn reference phases (Figure 4). All LDH phases were completely dissolved at pH 3.0. The time needed to dissolve 50% of the respective phase was 2.84 min for the pure Zn-LDH, 150 min for the mixed phase, and 1600 min for the pure Ni-LDH phase. Thus, the pure Zn-LDH dissolved much faster than the pure Ni-LDH, while the mixed ZnNi-LDH dissolved at an intermediate rate.

During acidification of the Zn- and Ni-only soil columns, a much larger fraction of the Zn-LDH than the Ni-LDH

dissolved. In the mixed-metal column, slightly less Zn was released, but significantly more Ni (Figure 3), while the relative fractions of Zn and Ni release were very similar (90% and 87% of the nonexchangeable amounts, respectively, Table 1). These observations can be rationalized considering the dissolution kinetics of the synthetic LDH references. The time needed for the dissolution of 50% of the synthetic Zn-LDH was 2.8 min. In the column experiment, the whole acidification step took 1500 min (0.5 min/pore volume). Thus, Zn in the Zn-only column dissolved relatively fast, and its release curve can be explained by a rapid dissolution followed by transport through the soil column. This transport is retarded by the readsorption of Zn to the soil matrix and is coupled to the breakthrough of the pH front, which in turn is retarded as a result of the dissolution of the precipitate phase and the protonation of the soil surface. Similar release curves were previously reported for the release of Zn from column acidification experiments with contaminated soils (48). In the case of the synthetic Ni-LDH, about 46% was dissolved within the duration of the acidification step in the column experiment (1500 min). This compares well to the release of 23% of the nonexchangeable Ni from the Ni-only column during acidification, considering that the dissolution was delayed by the retardation of the pH front. The release of Ni from the Ni-only column thus can be explained by an initial accumulated release peak coupled to the breakthrough of the acidification front and subsequent release at low concentration levels controlled by the rate of precipitate dissolution. The dissolution of 50% of the synthetic ZnNi-LDH took 150 min, i.e., 53 times longer than the dissolution of 50% of the Zn-LDH. Since the soil-formed ZnNi precipitate contained a higher fraction of Zn than the synthetic LDH phase, the difference in dissolution rate is expected to be smaller between the soil-formed Zn-only and ZnNi precipitates. The dissolution of the soil-formed ZnNi phase is therefore likely still fast compared to the duration of the leaching experiment, and the curves of Zn and Ni release can be interpreted in analogy to the Zn release from the Zn-only column. The delay in the release of Zn as compared to that of the Zn-only experiment (Figure 2) is due to the stronger retardation of the pH front, which again is caused by the larger amount of precipitate to be dissolved.

Environmental Implications. The results of this study demonstrate that the formation rate and composition of LDH-type precipitates in soils depend on the rates at which different cations present in the system enter into the LDH structure. The reactivity of the resulting precipitate depends on its composition and differs from the properties of LDH phases containing only one type of bivalent cation. Our results also show that the reactivity of such precipitates may not necessarily be inferred from the extent and rate at which they form. Cations which form sparingly soluble LDH precipitates may precipitate into more labile mixed LDH precipitates in the presence of other cations which form labile LDH phases. Rapidly forming LDH phases may readily dissolve again under more acidic conditions, while slowly forming precipitates may be more recalcitrant to dissolution. These phenomena need to be considered if metal retention by LDH precipitates is to be included in risk assessment and reactive transport modeling. The present study considered the case of Zn and Ni, but we expect that our findings are more generally applicable to the bivalent trace metals Ni²⁺, Co²⁺, and Zn²⁺ and the major cations Mg²⁺ and Fe²⁺ in LDH structures.

Acknowledgments

We thank Sabina Pfister for synthesizing the Zn-LDH, Ni-LDH, and ZnNi-LDH reference phases and Kurt Barmettler for his support in the laboratory. We acknowledge Andreas C. Scheinost for providing the EXAFS spectra of Ni-phyllo-

silicate and α - and β -Ni(OH)₂ and Darryl R. Roberts for the EXAFS data of amorphous Zn(OH)₂. The Angströmquelle Karlsruhe is acknowledged for providing beamtime at the XAS beamline. We thank Kumi Pandya from beamline X11A at NSLS, Stephan Mangold from the XAS beamline at ANKA, and Harald Funke from the ROBL beamline at ESRF for their support with EXAFS measurements. Finally, we acknowledge the four anonymous reviewers and the associate editor for their constructive comments. This research was financially supported by the Swiss Federal Institute of Technology (ETH), Zurich, under Contract No. 0-20966-02.

Supporting Information Available

Complete results from a six-step sequential extraction of Al, Fe, and Mn from the soil used in this study, XRD spectra of the synthetic LDH reference phases, and back-transform EXAFS spectra of Zn and Ni in Ca-extracted soil samples and in LDH-, phyllosilicate-, and hydroxide-type layered reference phases. This material is available free of charge via the Internet at <http://pubs.acs.org>.

Literature Cited

- Alloway, B. J., Ed. *Heavy Metals in Soils*; Chapman & Hall: London, 1995.
- Trivedi, P.; Axe, L. Predicting divalent metal sorption to hydrous Al, Fe, and Mn oxides. *Environ. Sci. Technol.* **2001**, *35*.
- McBride, M. B. In *Handbook of Soil Science*; Sumner, M. E., Ed.; CRC Press: Boca Raton, FL, 1999; pp B/265–B/302.
- Roberts, D. R.; Ford, R. G.; Sparks, D. L. Kinetics and mechanisms of Zn complexation on metal oxides using EXAFS spectroscopy. *J. Colloid Interface Sci.* **2003**, *263*, 364–376.
- Scheinost, A. C.; Ford, R. G.; Sparks, D. L. The role of Al in the formation of secondary Ni precipitates on pyrophyllite, gibbsite, talc, and amorphous silica: A DRS study. *Geochim. Cosmochim. Acta* **1999**, *63*, 3193–3203.
- Scheinost, A. C.; Sparks, D. L. Formation of layered single- and double metal hydroxide precipitates at the mineral/water interface: A multiple-scattering XAFS analysis. *J. Colloid Interface Sci.* **2000**, *223*, 167–178.
- Trainor, T. P.; Brown, G. E., Jr.; Parks, G. A. Adsorption and precipitation of aqueous Zn(II) on alumina powders. *J. Colloid Interface Sci.* **2000**, *231*, 359–372.
- Ford, R. G.; Sparks, D. L. The nature of Zn precipitates formed in the presence of pyrophyllite. *Environ. Sci. Technol.* **2000**, *34*, 2479–2483.
- Scheidegger, A. M.; Lamble, G. M.; Sparks, D. L. Investigation of Ni sorption on pyrophyllite: An XAFS study. *Environ. Sci. Technol.* **1996**, *30*, 548–554.
- Scheidegger, A. M.; Lamble, G. M.; Sparks, D. L. Spectroscopic evidence for the formation of mixed-cation hydroxide phases upon metal sorption on clays and aluminum oxides. *J. Colloid Interface Sci.* **1997**, *186*, 118–128.
- Scheidegger, A. M.; Strawn, D. G.; Lamble, G. M.; Sparks, D. L. The kinetics of mixed Ni–Al hydroxide formation on clay and aluminium oxide minerals: A time-resolved XAFS study. *Geochim. Cosmochim. Acta* **1998**, *62*, 2233–2245.
- Schlegel, M. L.; Manceau, A.; Charlet, L.; Chateignier, D.; Hazeman, J. Sorption of metal ions on clay minerals III. Nucleation and epitaxial growth of Zn phyllosilicates on the edges of hectorite. *Geochim. Cosmochim. Acta* **2001**, *65*, 4155–4170.
- Dähn, R.; Scheidegger, A. M.; Manceau, A.; Schlegel, M. L.; Baeyens, B.; Bradbury, M. H.; Morales, M. Neof ormation of Ni phyllosilicate upon Ni uptake on montmorillonite: A kinetics study by powder and polarized extended X-ray absorption fine structure spectroscopy. *Geochim. Cosmochim. Acta* **2002**, *66*, 2335–2347.
- Charlet, L.; Manceau, A. Evidence for the neof ormation of clays upon sorption of Co(II) and Ni(II) on silicates. *Geochim. Cosmochim. Acta* **1994**, *58*, 2577–2582.
- Voegelin, A.; Scheinost, A. C.; Bühlmann, K.; Barmettler, K.; Kretzschmar, R. Slow formation and dissolution of Zn precipitates in soil: A combined column-transport and XAFS study. *Environ. Sci. Technol.* **2002**, *36*, 3749–3754.
- Roberts, D. R.; Scheidegger, A. M.; Sparks, D. L. Kinetics of mixed Ni–Al precipitate formation on a soil clay fraction. *Environ. Sci. Technol.* **1999**, *33*, 3749–3754.

- (17) Manceau, A.; Lanson, B.; Schlegel, M. L.; Harge, J. C.; Musso, M.; Eybert-Berard, L.; Hazemann, J.-L.; Chateigner, D.; Lambelle, G. M. Quantitative Zn speciation in smelter-contaminated soils by EXAFS spectroscopy. *Am. J. Sci.* **2000**, *300*, 289–343.
- (18) Juillot, F.; Morin, G.; Ildefonse, P.; Trainor, T. P.; Benedetti, M.; G., L.; Calas, G.; Brown, G. E. Occurrence of Zn/Al hydroxalcalite in smelter-impacted soils from northern France: Evidence from EXAFS spectroscopy and chemical extractions. *Am. Mineral.* **2003**, *88*, 509–526.
- (19) Allada, R. K.; Navrotsky, A.; Berbeco, H. T.; Casey, W. H. Thermochemistry and aqueous solubilities of hydroxalcalite-like solids. *Science* **2002**, *296*, 721–723.
- (20) Boclair, J. W.; Braterman, P. S. Layered double hydroxide stability. I. Relative stabilities of layered double hydroxides and their simple counterparts. *Chem. Mater.* **1999**, *11*, 298–302.
- (21) Johnson, C. A.; Glasser, F. P. Hydroxalcalite-like minerals ($M_2\text{-Al}(\text{OH})_6(\text{CO}_3)_{0.5}\text{XH}_2\text{O}$, where M = Mg, Zn, Co, Ni) in the environment: Synthesis, characterization and thermodynamic stability (vol 51, pg 1, 2003). *Clays Clay Miner.* **2003**, *51*, 357–357.
- (22) Ford, R. G.; Scheinost, A. C.; Scheckel, K. G.; Sparks, D. L. The link between clay mineral weathering and the stabilization of Ni surface precipitates. *Environ. Sci. Technol.* **1999**, *33*, 3140–3144.
- (23) Eick, M. J.; Naprstek, B. R.; Brady, P. V. Kinetics of Ni(II) sorption and desorption on kaolinite: Residence time effects. *Soil Sci.* **2001**, *166*, 11–17.
- (24) Scheckel, K. G.; Sparks, D. L. Kinetics of the formation and dissolution of Ni precipitates in a gibbsite/amorphous silica mixture. *J. Colloid Interface Sci.* **2000**, *229*, 222–229.
- (25) Scheckel, K. G.; Scheinost, A. C.; Ford, R. G.; Sparks, D. L. Stability of layered Ni hydroxide surface precipitates—A dissolution kinetics study. *Geochim. Cosmochim. Acta* **2000**, *64*, 2727–2735.
- (26) Elzinga, E. J.; Sparks, D. L. Nickel sorption mechanisms in a pyrophyllite-montmorillonite mixture. *J. Colloid Interface Sci.* **1999**, *213*, 506–512.
- (27) Yamaguchi, N. U.; Scheinost, A. C.; Sparks, D. L. Surface-induced nickel hydroxide precipitation in the presence of citrate and salicylate. *Soil Sci. Soc. Am. J.* **2001**, *65*, 729–736.
- (28) Yamaguchi, N. U.; Scheinost, A. C.; Sparks, D. L. Influence of gibbsite surface area and citrate on Ni sorption mechanisms at pH 7.5. *Clays Clay Miner.* **2002**, *50*, 784–790.
- (29) Nachtegaal, M.; Sparks, D. L. Nickel sequestration in a kaolinite-humic acid complex. *Environ. Sci. Technol.* **2003**, *37*, 529–534.
- (30) Voegelin, A.; Vulava, V. M.; Kretzschmar, R. Reaction-based model describing sorption and transport of Cd, Zn, and Ni in an acidic soil. *Environ. Sci. Technol.* **2001**, *35*, 1651–1657.
- (31) Schwartz, A.; Wilcke, W.; Stýk, J.; Zech, W. Heavy metal release from soil in batch pHstat experiments. *Soil Sci. Soc. Am. J.* **1999**, *63*, 290–296.
- (32) Zeien, H.; Brümmner, G. W. Chemische Extraktion zur Bestimmung von Schwermetallbindungsformen in Böden. *Mitt. Dtsch. Bodenk. Ges.* **1989**, *59*, 505–510.
- (33) Martell, A. E.; Smith, R. M.; Motekaitis, R. J. *NIST Database 46, Critically Selected Stability Constants of Metal Complexes*, Version 6.0; National Institute of Standards and Technology: Gaithersburg, MD, 1997.
- (34) Taylor, R. M. The rapid formation of crystalline double hydroxy salts and other compounds by controlled hydrolysis. *Clay Miner.* **1984**, *19*, 591–603.
- (35) Lytle, F. W.; Sandstrom, D. R.; Marques, E. C.; Wong, J.; Spiro, C. L.; Huffman, G. P.; Huggins, F. E. Measurement of soft X-ray absorption spectra with a fluorescence ion chamber detector. *Nucl. Instrum. Methods Phys. Res.* **1984**, *226*, 542–548.
- (36) Matz, W.; Schell, N.; Bernhard, G.; Prokert, F.; Reich, T.; Claussner, J.; Oehme, W.; Schlenk, R.; Diemel, S.; Funke, H.; Eichhorn, F.; Betzl, M.; Pröhl, D.; Strauch, U.; Hüttig, G.; Krug, H.; Neumann, W.; Brendler, V.; Reichel, P.; Denecke, M. A.; Nitsche, H. ROBL—a CRG beamline for radiochemistry and materials research at the ESRF. *J. Synchrotron Radiat.* **1999**, *6*, 1076–1085.
- (37) Ressler, T. WinXAS: a program for X-ray absorption spectroscopy data analysis under MS—Windows. *Journal of Synchrotron Radiation* **1998**, *5*, 118–122.
- (38) Rehr, J. J. *FEFF: Ab initio multiple scattering X-ray absorption fine structure and X-ray absorption near edge structure code*, 7.02 ed.; FEFF Project, Department of Physics, University of Washington: Seattle, Washington, 1996.
- (39) O'Day, P.; Rehr, J. J.; Zabinsky, S. I.; Brown, G. E., Jr. Extended X-ray absorption fine structure (EXAFS) analysis of disorder and multiple-scattering in complex crystalline solids. *J. Am. Chem. Soc.* **1994**, *116*, 2938–2949.
- (40) Scheinost, A. C.; Kretzschmar, R.; Pfister, S.; Roberts, D. R. Combining selective sequential extractions, X-ray absorption spectroscopy, and principal component analysis for quantitative zinc speciation in soil. *Environ. Sci. Technol.* **2002**, *36*, 5021–5028.
- (41) Manceau, A.; Marcus, M. A.; Tamura, N.; Proux, O.; Geoffroy, N.; Lanson, B. Natural speciation of Zn at the micrometer scale in a clayey soil using X-ray fluorescence, absorption, and diffraction. *Geochim. Cosmochim. Acta* **2004**, *68*, 2467–2483.
- (42) d'Espinose de la Caillerie, J.-B.; Kermarec, M.; Clause, O. Impregnation of gamma-alumina with Ni(II) and Co(II) ions at neutral pH: Hydroxalcalite-type coprecipitate formation and characterization. *J. Am. Chem. Soc.* **1995**, *117*, 11471–11481.
- (43) Towle, S. N.; Bargar, J. R.; Brown, G. E.; Parks, G. A. Surface precipitation of Co(II)(aq) on Al_2O_3 . *J. Colloid Interface Sci.* **1997**, *187*, 62–82.
- (44) Thompson, H. A.; Parks, G. A.; Brown, G. E., Jr. Dynamic interactions of dissolution, surface adsorption, and precipitation in an aging cobalt(II)-clay-water system. *Geochim. Cosmochim. Acta* **1999**, *63*, 1767–1779.
- (45) Thompson, H. A.; Parks, G. A.; Brown, G. E. J. Formation and release of cobalt(II) sorption and precipitation products in aging kaolinite-water slurries. *J. Colloid Interface Sci.* **2000**, *222*, 241–253.
- (46) Kinniburgh, D. G.; Jackson, M. L.; Syers, J. K. Adsorption of alkaline earth, transition, and heavy metal cations by hydrous oxide gels of iron and aluminum. *Soil Sci. Soc. Am. J.* **1976**, *40*, 796–799.
- (47) Stumm, W.; Morgan, J. J. *Aquatic Chemistry*; John Wiley and Sons: New York, 1996.
- (48) Voegelin, A.; Barmettler, K.; Kretzschmar, R. Heavy metal release from contaminated soils: Comparison of column leaching and batch extraction results. *J. Environ. Qual.* **2003**, *32*, 865–875.

Received for review January 3, 2005. Revised manuscript received April 19, 2005. Accepted May 2, 2005.

ES0500097